frontiers in Environmental Science

ORIGINAL RESEARCH
published: 30 July 2020
doi: 10.3389/fenvs.2020.00114

Geochemistry of Engineered Nanoparticles (CdSe/ZnS Quantum Dots) in Surface Waters

*N. Izyan Supiandi, Rute F. Domingos, Marc F. Benedetti and Yann Sivry**

Institut de Physique du Globe de Paris, Université de Paris, CNRS UMR7154, Paris, France

The difficulties when studying the behavior of engineered nanoparticles (ENPs), and the subsequent metal speciation in aquatic ecosystems, at environmentally relevant concentrations (i.e., ppt level) are often related to the occurrence of ENP constitutive elements at high concentrations as a background in aquatic media. In this study, the physicochemical behavior of CdSe/ZnS quantum dots (QDs) when spread at very low concentrations in surface waters was investigated. The above-mentioned issues were overcome with the use of isotopically labeled QDs, separated by centrifugal ultrafiltration (CU) and measured by high-resolution inductively coupled plasma mass spectrometry (HR-ICP-MS), combined with the detection of free and labile metal ions by scanned stripping chronopotentiometry (SSCP). They firmly provided a thorough comprehension regarding the transformation of QDs in surface waters. The physicochemical conditions of the medium including the presence of an analog of natural organic matter and a mineral (i.e., fulvic acid and goethite), the manufactured coating of the QDs [here thioglycolic acid (TGA)], and the occurrence of added Zn in the medium were considered in the study. The overall results show that, in the absence of mineral/organic matter, the TGA ligands in solution that detached from the QD surface after dissolution control the metal speciation, especially for Cd. Conversely, in a more representative aquatic ecosystem condition (i.e., with Zn in the background media together with fulvic acid and goethite), almost no Zn or Cd dissolution from the QDs is detected. SSCP measurements reveal that the Zn complexes formed with the organic/mineral material in the system are inert, whereas the speciation model calculations indicated that Cd^{2+} is bound to TGA ligands in solution and organic/inorganic matter—therefore suggesting that, under the studied conditions, aquatic organisms will be exposed to a very low concentration of free and labile metal ions issued from the QDs.

Keywords: quantum dots, isotopic labeling, speciation, surface waters, dissolution, zinc, cadmium

OPEN ACCESS

Edited by:
Vera I. Slaveykova, Université de Genève, Switzerland

Reviewed by:
Claude Fortin, Institut National de la Recherche Scientifique (INRS), Canada
Huacheng Xu, Nanjing Institute of Geography and Limnology (CAS), China

***Correspondence:**
Yann Sivry
sivry@ipgp.fr

Specialty section:
This article was submitted to Biogeochemical Dynamics, a section of the journal Frontiers in Environmental Science

Received: *31 March 2020*
Accepted: *29 June 2020*
Published: *30 July 2020*

Citation:
Supiandi NI, Domingos RF, Benedetti MF and Sivry Y (2020) Geochemistry of Engineered Nanoparticles (CdSe/ZnS Quantum Dots) in Surface Waters. Front. Environ. Sci. 8:114. doi: 10.3389/fenvs.2020.00114

INTRODUCTION

The progress of nanotechnology led to numerous applications of engineered nanoparticles (ENPs), which results in the increase of studies concerning their fate and behavior in environmental compartments (e.g., wastewater treatment plants, surface water, sediments, and soils), as well as their potential toxic effects. However, most of these studies are often carried out at conditions far

from the ones expected in the environment, mostly for two main reasons. Firstly, the concentrations of ENPs used are generally higher than those predicted or measured for aquatic ecosystems, i.e., micromolar vs nanomolar (Gottschalk et al., 2009; Piccinno et al., 2012), mostly due to the analytical detection limits but also to the difficulty in detecting these ENPs in complex matrices with high natural concentrations of ENP constitutive elements. Secondly, the presence of other metal ions and organic/mineral matter, which are key players for metal ion speciation, is much neglected, especially during the investigations of ENP effects on living organisms.

Nevertheless, it is known that changes in ENP concentration and the occurrence of other metal ions and mineral/organic matters can affect their behavior, and the speciation of metal ions from ENP dissolution can change due to metal ions binding to the mineral and organic matters. For example, it has been shown that the dissolution of ZnO nanoparticles (NPs) decreases with its increasing concentration (Yung et al., 2015) or that the presence of humic substances in aquatic systems results in less ZnO and TiO_2 NP homoaggregation due to their heteroaggregation, suggesting that NP dispersion should be stable in a natural environment (Domingos et al., 2009, 2013b). On the other hand, Cd and Pb metal ions were shown to interact with CdTe/CdS NPs, influencing their dissolution and metal ion speciation (Cd and Pb) and thus their environmental fate (Domingos et al., 2015).

To this day, studies have not yet investigated the fate of ENPs under environmentally relevant conditions for aquatic ecosystems (i.e., at predicted or measured ENP concentrations) and in the presence of organic/mineral matter and other metal ions as well. In this study, we characterized the fate of ENPs at low and environmentally relevant concentrations and identified the geochemical processes at work. We have specifically focused on (i) ENP stability (i.e., dissolution and its rate) in aquatic media and (ii) the phases (e.g., organic/mineral matter and ENPs constitutive elements) susceptible to control the fate of ENPs. Some environmental implications of the findings on ENP behavior for the aquatic ecosystems are discussed in this article.

To answer those questions, we decided to use CdSe/ZnS quantum dot (QD) ENPs. CdSe/ZnS QDs are highly representative of core/shell-structured ENPs; they are exponentially used for light conversion purposes (e.g., in devices and materials intended for display, photovoltaic, lighting, and sensors) as well as in laboratory use for imaging (Piccinno et al., 2012; Pickering et al., 2012; Zhao et al., 2012; Dai et al., 2017). Moreover, one of their constituting elements (i.e., Zn) has high background concentration values in most of the aquatic ecosystems (ppb level), which contrasts with the estimated concentration of Zn-containing ENPs (ppt level) in surface water (Piccinno et al., 2012; Gottschalk et al., 2015).

Batch experiments were performed, using mixtures of QDs and water with different chemical compositions and analogs of suspended matter to follow, as a function of time, the changes in chemical composition of the model surface waters. The use of isotopically modified (or "spiked") ENPs (Supiandi et al., 2019, 2020) with centrifugal ultrafiltration (CU) separation and detection by high-resolution inductively coupled plasma mass spectrometry (HR-ICP-MS) overcame the analytical barriers (detection limits and geochemical background) to obtain the metal ion concentration and origins in the dissolved fraction. The speciation of QDs constituting metal ions (Cd and Zn) in the experimental systems (Domingos et al., 2008) was followed by scanned stripping chronopotentiometry (SSCP).

MATERIALS AND METHODS

We used concentrations of QDs approaching the ENP predicted concentrations in the environment (nanomolar/ppt level), in the absence and presence of one organic and mineral suspended matter constituent (a fulvic acid and an iron oxide, namely, goethite), while also considering the absence and presence of Zn from the geochemical background.

Multi-Isotopically Labeled $^{111}Cd^{77}Se/^{68}ZnS$ QDs

The CdSe/ZnS QDs used in this study were enriched in ^{111}Cd, ^{77}Se, and ^{68}Zn. The chemicals used including the synthesis protocol and the characterization methods of the multi-spiked QDs were described in previous works (Supiandi et al., 2019, 2020). Briefly, a stock solution of the QDs in an organic phase was synthesized and used to prepare water-soluble QDs, i.e., functionalized with thioglycolic acid (TGA). A solution of TGA-coated QDs was used in the experiments carried out in this study.

Synthetic River Water

The choice was made to work with a synthetic water instead of a real natural water. Being the first study targeting such low concentrations of ENPs, therefore, it is of major concern to have full control of the water constituents that can have an impact on the QD fate and speciation. A synthetic river water (SRW), analog of the Seine river flowing in Paris (Hammes et al., 2013; Sivry et al., 2014), was prepared. $Ca(NO_3)_2$, Na_2SO_4, and NaHEPES salts were added into a known quantity of ultrapure water from Milli-Q Millipore (resistivity > 18 MΩ.cm) to obtain a 2 mM Ca^{2+} solution, buffered at pH 8 (1 mM of NaHEPES) and 0.56 mM of Na^+ and 0.28 mM of SO_4^{2-}. HEPES is assumed to be noncomplexing; therefore, it would not have implications on the speciation studies (Soares and Conde, 2000). Carbonates in the systems come from the equilibration with the atmosphere, since no specific effort was made to prevent CO_2 dissolution during the experiments. The ionic strength of the prepared SRW was approximately 7 mM.

Different components were then added to the SRW, to obtain a total of five different water conditions: (A) SRW; (B) SRW-Zn, SRW in which $Zn(NO_3)_2$ was added to reach a concentration of 60 nM; (C) SRW-Zn-FA, corresponding to SRW-Zn with an addition of Suwannee river fulvic acid to a concentration of 5 ppm (SRFA; from the International Humic Substances Society, noted as FA hereafter); (D) SRW-Zn-G corresponding to SRW-Zn with an addition of goethite to reach 20 ppm of concentration. The goethite was prepared according to Hiemstra et al. (1989), and its characterization can be found in Zelano et al. (2016); and (E) SRW-Zn-FA-G, corresponding to SRW-Zn with an addition of FA (5 ppm) and goethite (20 ppm). The concentrations of these

components are relevant in most natural river systems (Hammes et al., 2013; Sivry et al., 2014).

Batch Experiments

The dissolution and speciation of the QD constituting elements (Zn and Cd) in synthetic waters A, B, C, D, and E were followed for 8 days, at different intervals of time (t = 0, 2, 6, 24, 48, 96, 144, and 192 h). The initial QD concentrations used were relevant to the estimated ENP concentrations found in the environment, i.e., ppt–ppb level (Gottschalk et al., 2009; Piccinno et al., 2012), and significantly higher than the limit of quantification (LOQ) previously determined for the isotopically labeled QDs spread in natural waters (i.e., QD-LOQ, Supiandi et al., 2019). For each time step and for both dissolution and speciation experiments, 20 ml of each water sample was prepared in a disposable polystyrene cup. The concentration of QDs added at t = 0 in each cup was to reach 7.6 nM of Zn (500 ppt), corresponding to 1.4 nM of Cd (160 ppt) and 0.8 nM of Se (63 ppt). For the latter, this concentration is too close to the HR-ICP-MS LOQ (60 ppt) to obtain reliable data. Therefore, only Zn and Cd results are discussed hereafter. To summarize the batch experiments, the dissolution of the QDs in each cup was followed by CU and HR-ICP-MS analysis; meanwhile, the speciation was studied using SSCP; both methods are detailed hereafter.

Besides, electrophoretic mobility (EPM) measurements of QDs and organic and mineral matter in waters A, B, C, D, and E were also carried out using a Malvern Zetasizer Nano-ZS (Malvern, DTS1061) at 20°C. Each sample value corresponds to the mean of at least five independent measurements. The standard DTS1235 for zeta potential was used after every ∼10 measurements to verify the performance of the system.

CU + HR-ICP-MS

Centrifugal filter units (Amicon® Ultra Centrifugal Filter Units, 3 kDa cutoff equivalent to 1–2 nm pore diameters) were used to separate QDs from free Zn and Cd ions as well as complexes resulting from QD dissolution with a smaller size than the cutoff. At different time intervals (t = 0, 2, 6, 24, 48, 96, 144, and 192 h), 4 ml of QD-containing solutions (from conditions A–E) was sampled and centrifuged for 35 min at 3,220 g. The filtrates were collected and acidified (2% of HNO_3 in solution) prior to analysis by HR-ICP-MS. The concentrations of spiked Zn and Cd in the CU dissolved fraction were calculated using the equations adapted from Dybowska et al. (2011) (see **Supplementary Material**), which allowed us to trace the dissolved metal released from the spiked ENPs, notwithstanding the high background concentrations, especially in Zn. The potential bias caused by CU on metal concentration due to the progressive and relative increase in large binding ligands while the volume of solution decreases over a 35 min period has been assessed in a previous study and found negligible in the experimental conditions fixed (Sivry et al., 2014). In addition, the information on the dissolution of isotopically labeled QDs is contained on the isotopic composition of the dissolved fraction, not on the concentration of the latter. Therefore, the use of isotopically labeled QDs allows us to get rid of a potential adsorption of dissolved metal on the membrane or on the walls of the CU cell.

External standard solutions containing 1, 5, 10, 100, 500, 1,000, and 5,000 ppt of total Cd and Zn were prepared in 2% HNO_3 and used for the HR-ICP-MS analyses. A solution containing 5 ppb of rhodium (^{103}Rh) prepared in 2% HNO_3 was used as an internal standard solution to correct from instrumental drift and mass bias. The isotopes of Cd (^{106}Cd, ^{108}Cd, ^{110}Cd, ^{111}Cd, ^{112}Cd, ^{113}Cd, ^{114}Cd, and ^{116}Cd) and Zn (^{64}Zn, ^{66}Zn, ^{67}Zn, ^{68}Zn, and ^{70}Zn) were analyzed with HR-ICP-MS. The isotopes ^{105}Pd, ^{115}In, ^{118}Sn, ^{60}Ni, and ^{72}Ge were also analyzed to correct for possible isobaric interferences. Each intensity used for data treatment corresponds to the average of 15 blocks of three replicates, allowing an internal reproducibility with a standard error better than 5%. Within each measurement sequence, reproducibility of the in-house multielement isotopic reference material (TM-23.4 Lake Ontario water from National Research Council Canada) was monitored at the beginning and the end of each analysis sequence, yielding less than 10% shift from the certified values. All results are presented as the mean and standard deviation of three replicates when available; meanwhile, results from single-replicated samples are presented as the mean and standard deviation of measurements of the 15 blocks of three replicates (standard error <5%).

Zn Speciation in Solution by SSCP

According to Merdzan et al. (2014), it is necessary to complement the CU data with other techniques to fully understand the behavior of the ENPs in complex waters, since each technique measures a slightly different fraction of the metal. SSCP was used here to obtain information on the lability degree of the complexes by following SSCP shift in the half-wave deposition potential (Pinheiro and van Leeuwen, 2004). A full description of SSCP can be found in Domingos et al. (2013a) (see **Supplementary Material**).

Scanned stripping chronopotentiometry was performed on all solutions from conditions A–E using an Eco Chemie potentiostat PGSTAT 128N in conjunction with a Metrohm 663 VA stand and the NOVA 1.11 software. Electrodes included an Ag/AgCl reference electrode with a 0.1 M $NaNO_3$ salt bridge, a platinum counter electrode, and a thin mercury film electrode plated onto a rotating glassy carbon disk (1.9 mm diameter, Metrohm). Calibration solutions ($C = 1 \times 10^{-7}$ M, pH = 4) were prepared daily. All solutions were purged with nitrogen for 20 min prior to the voltammetric experiments, and the measurements were carried out at room temperature (18–20°C). During an SSCP analysis, the potential was held at a deposition potential of Zn (E_d) for the duration of the deposition time (t_d = 45 or 90 s), during which Zn was accumulated on the working electrode, with E_d held at −1.3, −1.13, −1.075, −1.23, −1.19, −1.25, −1.09, −1.17, −1.15, −1.115, −1.16, −1.21, −1.1, −1.14, −1.125, −1.3, −1.065, and −1.055 V. After the accumulation step, an oxidizing strip current, $I_s = 1 \times 10^{-6}$ A, was applied in quiescent solution until the potential reached a value sufficiently beyond the transition plateau (−0.2 V). The raw signal is a measurement of the variation of potential with time that is automatically converted to the dt/dE-vs-E format. The

Zn concentrations calculated from the measurement data are representing the sum of Zn^{2+} ions in solution and Zn^{2+} coming from labile Zn complexes.

Scanned stripping chronopotentiometry results are presented as the mean and standard deviation or range of minimum and maximum values of at least three measurement replicates performed on different days with freshly prepared samples.

Model Calculations

Visual MINTEQ software (version 3.1) was used to evaluate the thermodynamic speciation of Zn and Cd in all water conditions, i.e., binding to inorganic ligands, TGA, FA, and goethite (Sivry et al., 2014), complementing the results obtained by CU/HR-ICP-MS and SSCP for Zn (see **Supplementary Material** for modeling details, parameters, and assumptions).

RESULTS

Characterization of CdSe/ZnS QDs

The multi-spiked QDs exhibit a green emission centered at 540 nm with an emission full width at half maximum (FWHM) of 40 nm. The synthesized QDs are round-shaped, and some are slightly oval, with an average of ∼7.6 nm in size. Figures and detailed characterization results are provided in the **Supplementary Material**.

General Observation on the CU/HR-ICP-MS Data

Figure 1 shows the CU/HR-ICP-MS filtrate concentrations of Zn and Cd, hereafter denoted Zn_{QDs} and Cd_{QDs}, respectively. The QD dissolution profiles are presented as a function of time for conditions A–E. The ratio between Zn_{QDs} and Cd_{QDs} dissolved fraction concentrations [$(Zn_{QDs})/(Cd_{QDs})$] compared to the initial Zn and Cd concentration (i.e., added as QDs) ratio is given in **Figure 2** to test congruent vs incongruent release of the two constituting elements under the studied conditions.

In simplified media, in the absence of mineral/organic matter (conditions A and B), the concentrations of Zn and Cd dissolved from the QD shell and core, (Zn_{QDs}) and (Cd_{QDs}), respectively, increase slowly within 24 h of exposure time, and total dissolution of Zn_{QDs} and Cd_{QDs} was observed after 48 h of exposure. The variation of $(Zn_{QDs})/(Cd_{QDs})$ ratios in the function of time seems similar in both cases, indicating that the addition of extra Zn in condition B does not seem to affect the dissolution of the QDs. At the beginning of the interaction, the ratios are much higher than the initial one (50 vs 5) showing that Zn_{QDs} is preferentially released compared to the Cd_{QDs} that dissolves slowly. At $t = 2$ and 6 h, this ratio is higher in condition A, indicating a higher release in Zn_{QDs} compared to that of condition B. But in both cases, the ratio toward the end of the experiment is equal the initial one [$(Zn_{QDs})/(Cd_{QDs}) = 5$].

In the presence of organic matter analog (FA), i.e., condition C, Zn_{QDs} and Cd_{QDs} dissolved slowly and did not reach total dissolution even after 8 days. This could be explained by the protection of the QDs by the FA (Domingos et al., 2009; Oriekhova and Stoll, 2016). The FA is most probably surrounding the QD surface, conferring a much more negative environment and thus stabilizing the particle and slowing down their dissolution, which is coherent with the EPM data (**Figure 3**). The $(Zn_{QDs})/(Cd_{QDs})$ ratios are slightly higher but almost similar to that of condition B, also indicating that the Zn_{QDs} release is more favored than that of Cd_{QDs}. However, the ratio has a different profile toward the end of the interaction (t = 96–144 h), showing that the concentration of dissolved Zn_{QDs} or its complexes in solution is higher than that of the Cd_{QDs} if

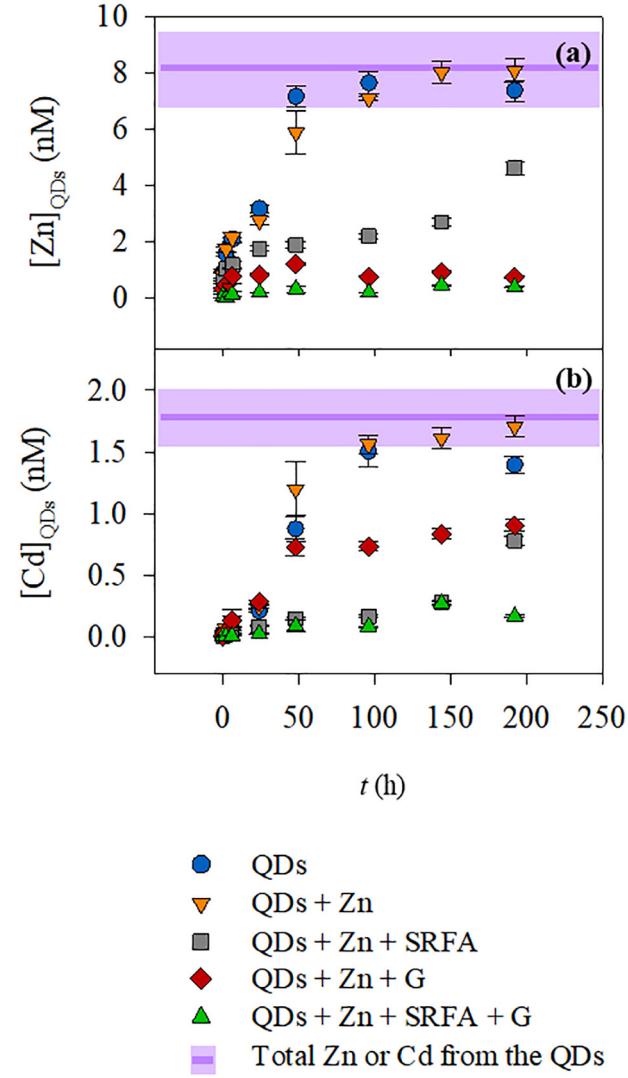

FIGURE 1 | Zn **(a)** and Cd **(b)** concentrations on the filtrates after CU as a function of time for the QDs dispersed in five different conditions: (●) QD dissolution in SRW; (▼) QD dissolution in SRW containing Zn (110 nM); (■) QD dissolution in SRW containing Zn and Suwannee river fulvic acid (FA, 5 ppm); (♦) QD dissolution in SRW containing Zn and goethite (G, 20 ppm); and (▲) QD dissolution in SRW containing Zn, FA, and G. The purple lines and shadowed areas represent the average and the standard deviation, respectively, of the total Zn or Cd of the QDs added at the beginning of the dissolution experiment.

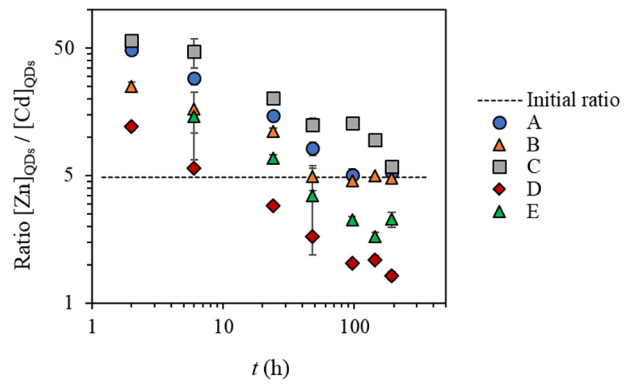

FIGURE 2 | The ratio between Zn_{QDs} and Cd_{QDs} dissolved fraction concentrations compared to the initial Zn_{QDs} and Cd_{QDs} concentration ratio in water conditions A–E. Conditions (A) SRW, (B) SRW-Zn, (C) SRW-Zn-FA, (D) SRW-Zn-G, and (E) SRW-Zn-FA-G.

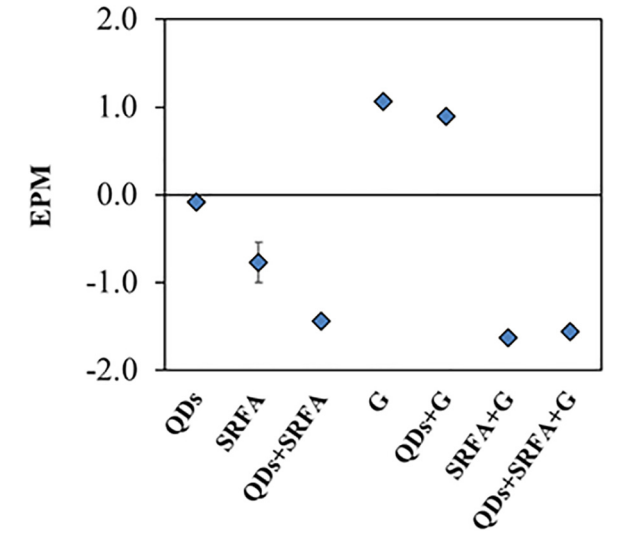

FIGURE 3 | EPM data obtained for the different samples containing only QDs, FA and goethite, and mixtures of them after 24 h of stabilization.

compared to conditions A and B. This can be explained by the speciation of Cd metal ions in the presence of FA, which are most probably forming complexes larger than the CU membrane cutoff. The ratio at 8 days (192 h) decreases to almost the initial one, indicating that the concentration of dissolved Cd_{QDs} in solution is identical to that of Zn_{QDs}.

In the presence of goethite mineral phase (condition D), almost no dissolved Zn_{QDs} shell was detected, but the release of the Cd_{QDs} core was observed. This indicates that the QD Zn shell should be totally dissolved, allowing the Cd core to dissolve unless the particles are highly porous. The absence of Zn in the CU filtrate indicates that Zn could be complexed by the goethite, which is much larger than the membrane pores. The presence of Cd in the filtrate suggests that goethite has a higher affinity for Zn compared to Cd, which was in fact previously shown (Spathariotis and Kallianou, 2007; Juillot et al., 2008). This can be seen from the dissolved $(Zn_{QDs})/(Cd_{QDs})$ ratios which are much lower compared to other conditions and especially lower than the initial ratio after 50 h of interaction, showing that dissolved Cd_{QDs} or its small complexes (<3 kDa) remain in solution after its release. However, the measured concentrations of dissolved Zn_{QDs} are lower than the LOQ of spiked QDs in surface waters found in our previous study, i.e., QD-LOQ_{Zn} = 1.4 nM = 95 ppt (Supiandi et al., 2019); therefore, the values of (Zn_{QDs}) in this condition are speculated to be unreliable.

In the presence of both FA and goethite (condition E), almost no dissolved Zn_{QDs} and Cd_{QDs} were observed, and the dissolved $(Zn_{QDs})/(Cd_{QDs})$ ratios are higher than those of conditions D, indicating that the release of Zn_{QDs} is more preferential. This can be explained by the speciation of Zn and Cd metal ions (forming complexes larger than the CU membrane cutoff) that will be verified later in this article.

Besides the information on the QD dissolution obtained from the CU/HR-ICP-MS, the overall data have shown in parallel the advantage of the ENP isotopic labeling technique when used with CU/HR-ICP-MS. The data of Zn particularly showed that the Zn dissolved from the QDs can be detected at nanomolar (ppt) level even in media with high-Zn background. The total concentration analysis by ICP-MS (not shown in the CU figures) indicated that the medium in condition A contains 51 nM of Zn in solution even without any initial addition of Zn as for the other waters, possibly due to the contamination coming from the various salts added for the preparation of the SRW. The media in conditions B–E contain about 110 nM of Zn resulting from the contamination plus the initial added Zn salt (60 nM). Even though these waters contain already almost 7–15 times higher Zn concentrations compared to the one coming from the QD [(Zn_{QDs}) = 7.4 nM], the dissolved Zn from the QDs was still quantified at such a low concentration.

DISCUSSION

Zn Lability

The SSCP data are presented separately for each condition (A–E) (**Figure 4**), showing the concentrations of labile Zn as a function of time. Overall, the labile Zn concentration (background + QDs) in all conditions decreases with time. However, in conditions D and E, the measured concentrations are much lower than those of conditions B and C, which have the same total Zn concentration initially added. This shows that the presence of goethite in the system influences the speciation of Zn, which most is probably forming strong complexes that are not easily dissociated, inducing much lower labile Zn concentrations.

The SSCP shift in the half-wave deposition potential ($\Delta E_{d,1/2}$) for all water conditions is presented altogether in **Figure 5**. Recall that $\Delta E_{d,1/2} = E_{d,1/2}$ (ML) $- E_{d,1/2}$ (M) is the difference of $E_{d,1/2}$ between the complexes (ML) and the free metals (M). For example, an increasing $|\Delta E_{d,1/2}|$ means formation of stronger labile complexes.

For conditions A and B, the values of $\Delta E_{d,1/2}$ are quite similar, indicating a formation of complexes with similar strength in both conditions, e.g., $ZnCO_3$, $ZnOH^+$, or ZnTGA. In the presence of

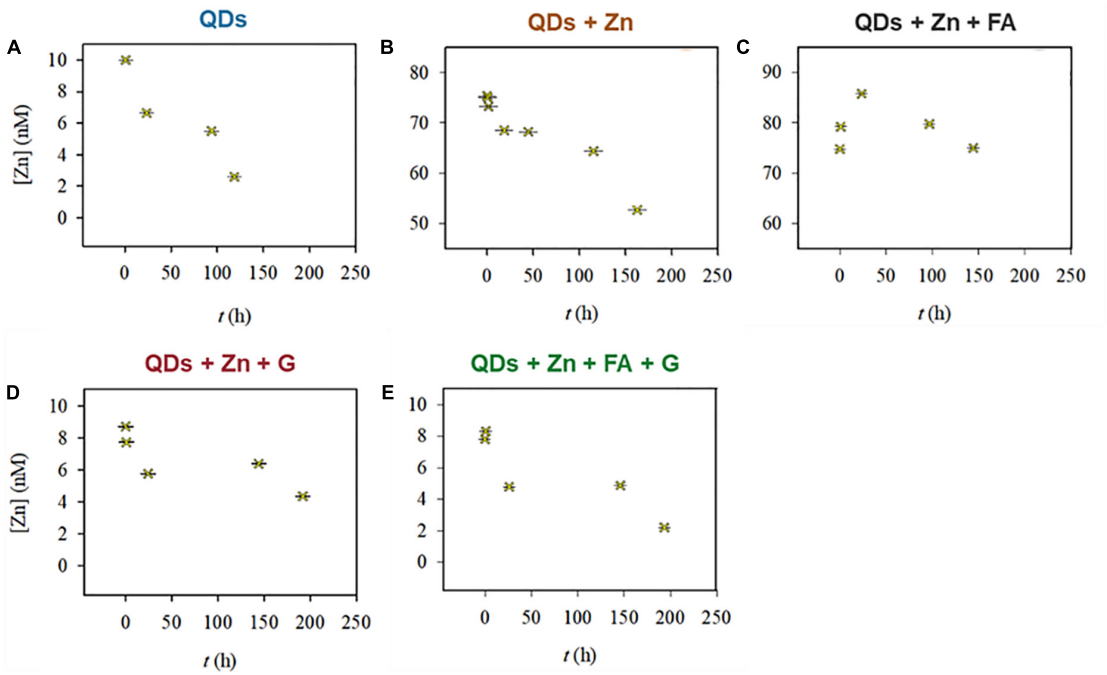

FIGURE 4 | Labile Zn concentrations in conditions **(A–E)**. Conditions **(A)** SRW, **(B)** SRW-Zn, **(C)** SRW-Zn-FA, **(D)** SRW-Zn-G, and **(E)** SRW-Zn-FA-G.

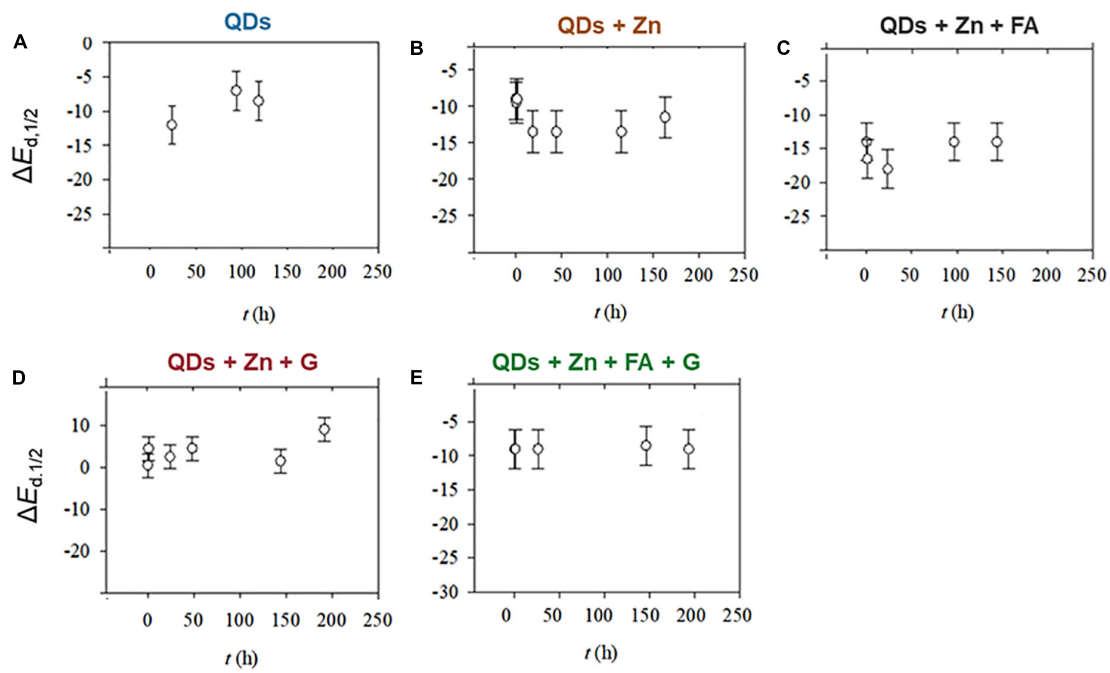

FIGURE 5 | Shift in the half-wave deposition potential, $\Delta E_{d,1/2}$, for conditions **(A–E)**. Conditions **(A)** SRW, **(B)** SRW-Zn, **(C)** SRW-Zn-FA, **(D)** SRW-Zn-G, and **(E)** SRW-Zn-FA-G.

FA (condition C), $|\Delta E_{d,1/2}|$ values are slightly higher than those of conditions A and B. This could be explained by the formation of slightly stronger complexes, e.g., ZnFA. In condition D (in the presence of goethite), the $\Delta E_{d,1/2}$ remained around 0, implying that the possible Zn complexes are inert, thus not possible to be measured. In fact, the SSCP wave (see **Supplementary Figure S3**) shows that the system is slightly heterogeneous (van Leeuwen and Town, 2003), indicating that Zn can be adsorbed

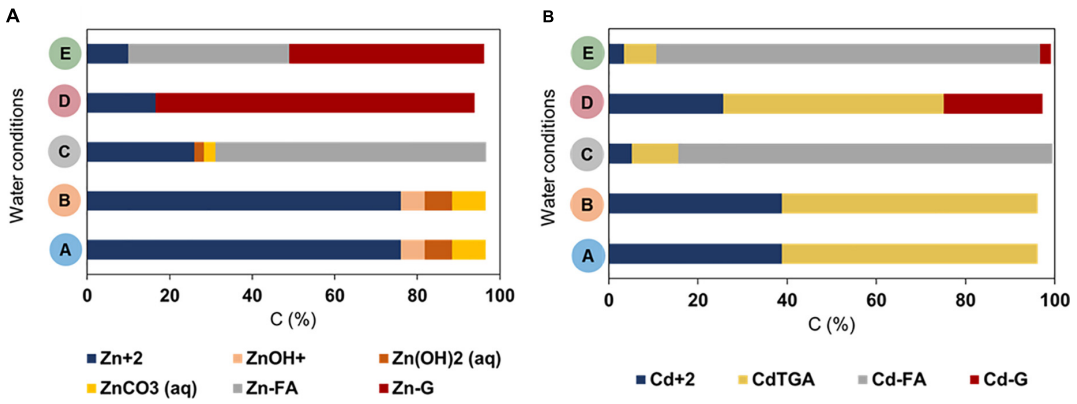

FIGURE 6 | Speciation of Zn **(A)** and Cd **(B)** by thermodynamic modeling. Conditions (A) SRW, (B) SRW-Zn, (C) SRW-Zn-FA, (D) SRW-Zn-G, and (E) SRW-Zn-FA-G.

by different binding sites of goethite particles. As for condition E (in the presence of both FA and goethite), the $\Delta E_{d,1/2}$ remained constant, but with a value around −10 mV compared to that of condition D (0 mV). Here, the FA impact can be seen with the formation of more labile complexes.

Zinc and Cadmium Speciation

The model calculations indicate that, under all studied conditions, the solid microsized CdSe, greenockite (CdS), and sphalerite (ZnS) are supposed to undergo total dissolution at equilibrium (see parameters in **Supplementary Table S8**). This is consistent with CU data of conditions A and B at the end of experiment, but not with the dissolution profile of conditions C–E from CU data that are not showing total dissolution. This can be explained by the speciation of Zn and Cd in each condition, presented in **Figure 6**. The concentrations of Zn^{2+} and Cd^{2+} decrease with the complexity of the water condition (A–E). In the absence of mineral and/or organic matter, Zn forms complexes with hydroxides and also few carbonates as shown previously by Sivry et al. (2014), in spite of the initial purge of the samples with nitrogen (see section "Zn Speciation in Solution by SSCP"), which highlights that the system is also equilibrating with atmospheric CO_2. TGA is known as a complexing agent for metal ions, e.g., Cd^{2+} and Hg^{2+} (Khatkar and Devi, 2006). However, there is less than 0.5% of ZnTGA complex formation according to the thermodynamic model. This is clearly related to the competition between Zn^{2+} and H^+ or Cd^{2+} to bind with TGA (log $K_{1,ZnTGA}$ = 7.8 vs log $K_{1,HTGA}$ = 10.3 and log $K_{1,CdTGA}$ = 11.5, see **Supplementary Table S1**). In addition, the complexes Cd forms with the TGA seem to be strong enough to not be detected during SCP. For all the conditions, the solutions were buffered at pH 8, in the range of pH with the largest binding capacity of TGA for the metal ions, in accordance with the first TGA dissociation constant (pKa_1 = 3.7, extrapolated to I = 0 M at 25°C; Domingos et al., 2015). The presence of Ca^{2+} in the medium does not induce any notable competition with Cd regarding its complexation with TGA (stability constants 1.5 vs 11.5, respectively, see **Supplementary Table S1**).

In a medium containing the organic matter analogue (FA, condition C, **Figure 6A**), Zn is shown to mostly complex with FA, but up to 30% remains free Zn^{2+}. On the contrary, 94% of Cd forms complex with organic matter (84% with FA and 10% with TGA, see **Supplementary Table S13**). However, in a medium with mineral matter (goethite, condition D, **Figure 6B**), Cd is mostly complexed with TGA rather than goethite (50% vs 22%), compared to Zn for which 77% is bound to goethite. These results are coherent with CU/HR-ICP-MS and SSCP data obtained previously: (i) the concentration of dissolved Cd_{QDs} in solution is higher than that of Zn_{QDs} in condition D since the CdTGA complexes are smaller than the CU membrane cutoff, and (ii) and Zn is not observed during SSCP, suggesting that its complexes with goethite are inert. Coherent with CU data, goethite has a higher affinity for Zn compared to Cd. When both mineral and organic matter are present in the medium, almost all Cd is bound to FA whereas Zn is complexed to both FA and goethite, which finally results in very low concentrations of Cd_{QDs} and Zn_{QDs} in solution since both are forming complexes bigger than 3 kDa. In addition, the model calculation (not shown here) indicates that FA surrounds the goethite surface forming very stable heteroaggregate, which is consistent with EPM data.

QD Fate in Surface Waters

The absence and the presence of mineral/organic matter in surface water analogs are shown to affect the speciation of Zn and Cd in solution, resulting in different QD core/shell dissolution profiles. CU data indicated a total dissolution of Zn shell and Cd core of the QDs after approximately 48 h when dispersed in simplified river water (in the absence of organic/inorganic phases but in the presence of natural Zn). However, the SSCP data showed a decrease in labile Zn concentrations with time. As for Cd, the presence of the TGA ligands in solution that detached from the QD surface after dissolution could potentially and strongly complex the Cd^{2+} metal ions, since no significant degradation of TGA itself is expected in these physicochemical conditions and timescale (De Villiers et al., 1997). No further SCP was applied for Cd due to the low concentration in Cd of the QDs used in this study, thus reaching the limit of detection of

the technique (0.05 nM, i.e., 5 ppt). However, model calculations showed that CdTGA complexes are the majority species of Cd in all studied water conditions, except when in the presence of organic matter analog FA since Cd^{2+} is mostly bound to FA binding sites.

Contrary to simplified systems, when the QDs were dispersed in a more representative aquatic system, i.e., in the presence of Zn, fulvic acids, and goethite, almost no Zn or Cd dissolution from the QDs was observed. The concentration of labile Zn measured was also very low compared to the one measured in simplified systems, yet still decreasing with time. In addition, the SSCP data reveal that the Zn complexes formed with the organic/inorganic matter in the system are strong/inert, whereas the CU/SCP/modeling data of Cd suggest its binding to the TGA ligands and FA (thus also FA–goethite heteroaggregates)—therefore suggesting that, under the conditions studied, aquatic organisms could be exposed to a lower concentration of free and labile metal ions coming from the QDs, therefore having less bioavailability and toxicity to water column organisms.

CONCLUSION

The difficulties when studying the fate of QDs in aquatic water systems at ppt-level concentrations and the subsequent metal speciation were surmounted by the combination of the two mentioned methods, isotopically labeled QDs/CU and SSCP. They firmly provided a thorough comprehension regarding the transformation of QDs in the environment, despite the low concentration used. The QD behavior in aquatic systems is affected by various factors: (i) the physicochemical conditions of the medium including the presence of natural organic and mineral matter, (ii) the presence of the manufactured coating of the QDs, and (iii) the interaction of the metal ions in the medium with the coating itself. For instance, the CU data indicated a total dissolution of Zn shell and Cd core of the QDs after approximately 48 h when dispersed in simplified river water (in the absence of organic/inorganic phases but in the presence of naturally occurring Zn). However, the SSCP data showed that these Zn and Cd are forming complexes with time, whose strength is stronger than the ones present in the system at the initial state, namely, the QD structure itself or some metal bound to the TGA present at the QD surface. In fact, the overall results seem to indicate that the presence of the TGA ligands in solution detached from the QD surface after dissolution could strongly complex the metal ions. Indeed, at pH 8, the largest binding capacity for the metal ions is expected, in accordance with the TGA dissociation constants: $pKa_1 = 3.7$ and $pKa_2 = 10.3$. As for Cd, no further SSCP was applied due to the low Cd concentration of the QDs used, thus reaching the limit of detection of the technique (5 ppt).

Contrary to when dispersed in a more representative aquatic system, i.e., in the presence of Zn, fulvic acids, and goethite, almost no Zn or Cd dissolution from the QDs was observed. The concentration of free and labile Zn measured was also very low compared to the one measured in the simplified system, yet still decreasing with time. In addition, the SSCP data reveal that the Zn complexes formed with the organic/inorganic matter in the system are inert, suggesting less concern regarding their bioavailability and toxicity to water column organisms, but the opposite for organisms in the sediment's top layer, such as filter feeds, due to the possible sedimentation of these inert complexes.

The unusual approach where two different yet complementary techniques were combined has surpassed the analytical limitations when studying the fate of ENPs at relevant concentrations, while simultaneously giving a detailed understanding regarding dynamic speciation. Precisely, without applying the isotopic labeling technique, dissolved ENPs would not be observed using the CU/HR-ICP-MS when working at very low concentrations in a complex system containing high background noise. The exact speciation of the ENPs under environmentally relevant conditions (i.e., with the presence of other metals and organic/inorganic matter) can be eventually determined with the coupling of isotopically labeled ENPs with CU/HR-ICP-MS and SSCP.

DATA AVAILABILITY STATEMENT

All datasets presented in this study are included in the article/**Supplementary Material**.

AUTHOR CONTRIBUTIONS

NS was in charge of all the experiments, analyses, and writing. NS was supervised and guided by RD for the SSCP experiments and data treatment. YS conceived the presented idea and coordinated and supervised the whole work. MB helped him supervise the project. All authors discussed and wrote the final manuscript.

FUNDING

This research project was co-financed by the French Agency for Food, Environmental and Occupational Health and Safety (ANSES) under the convention nos. EST-2013/1/264 and the ANR-18-IDEX-0001, IdEx Université de Paris. Part of this work was supported by the IPGP multidisciplinary program PARI and by Paris-IdF region SESAME grant no. 12015908.

ACKNOWLEDGMENTS

Our thanks go to Ms. Laure Cordier and M. Mickaël Tharaud for the assistance they provided during various multielemental analyses and to Dr. Gaëlle Charron for supervising the synthesis of this QD batch.

SUPPLEMENTARY MATERIAL

The Supplementary Material for this article can be found online at: https://www.frontiersin.org/articles/10.3389/fenvs.2020.00114/full#supplementary-material

REFERENCES

Dai, X., Deng, Y., Peng, X., and Jin, Y. (2017). Quantum-dot light-emitting diodes for large-area displays: towards the dawn of commercialization. *Adv. Mater. Weinheim* 29:1607022. doi: 10.1002/adma.201607022

De Villiers, M., Wurster, D. E., and Narsai, K. (1997). Stability of lactic acid and glycolic acid in aqueous systems subjected to acid hydrolysis and thermal decomposition. *J. Cosm. Sci.* 48, 165–174.

Domingos, R. F., Franco, C., and Pinheiro, J. P. (2013a). Stability of core/shell quantum dots—role of pH and small organic ligands. *Environ. Sci. Pollut. Res.* 20, 4872–4880. doi: 10.1007/s11356-012-1457-0

Domingos, R. F., Franco, C., and Pinheiro, J. P. (2015). The role of charged polymer coatings of nanoparticles on the speciation and fate of metal ions in the environment. *Environ. Sci. Pollut. Res. Int.* 22, 2900–2906. doi: 10.1007/s11356-014-3546-8

Domingos, R. F., Huidobro, C., Companys, E., Galceran, J., Puy, J., and Pinheiro, J. P. (2008). Comparison of AGNES (absence of gradients and Nernstian equilibrium stripping) and SSCP (scanned stripping chronopotentiometry) for trace metal speciation analysis. *J. Electroanal. Chem.* 617, 141–148. doi: 10.1016/j.jelechem.2008.02.002

Domingos, R. F., Rafiei, Z., Monteiro, C. E., Khan, M. A. K., and Wilkinson, K. J. (2013b). Agglomeration and dissolution of zinc oxide nanoparticles: role of pH, ionic strength and fulvic acid. *Environ. Chem.* 10, 306–312. doi: 10.1071/EN12202

Domingos, R. F., Tufenkji, N., and Wilkinson, K. J. (2009). Aggregation of titanium dioxide nanoparticles: role of a fulvic acid. *Environ. Sci. Technol.* 43, 1282–1286. doi: 10.1021/es8023594

Dybowska, A. D., Croteau, M.-N., Misra, S. K., Berhanu, D., Luoma, S. N., Christian, P., et al. (2011). Synthesis of isotopically modified ZnO nanoparticles and their potential as nanotoxicity tracers. *Environ. Pollut.* 159, 266–273. doi: 10.1016/j.envpol.2010.08.032

Gottschalk, F., Lassen, C., Kjoelholt, J., Christensen, F., and Nowack, B. (2015). Modeling flows and concentrations of nine engineered nanomaterials in the danish environment. *Int. J. Environ. Res. Public Health* 12, 5581–5602. doi: 10.3390/ijerph120505581

Gottschalk, F., Sonderer, T., Scholz, R. W., and Nowack, B. (2009). Modeled environmental concentrations of engineered nanomaterials (TiO2, ZnO, Ag, CNT, Fullerenes) for different regions. *Environ. Sci. Technol.* 43, 9216–9222. doi: 10.1021/es9015553

Hammes, J., Gallego-Urrea, J. A., and Hassellöv, M. (2013). Geographically distributed classification of surface water chemical parameters influencing fate and behavior of nanoparticles and colloid facilitated contaminant transport. *Water Res.* 47, 5350–5361. doi: 10.1016/j.watres.2013.06.015

Hiemstra, T., De Wit, J. C. M., and Van Riemsdijk, W. H. (1989). Multisite proton adsorption modeling at the solid/solution interface of (hydr)oxides: a new approach. *J. Coll. Interface Sci.* 133, 105–117. doi: 10.1016/0021-9797(89)90285-3

Juillot, F., Maréchal, C., Ponthieu, M., Cacaly, S., Morin, G., Benedetti, M., et al. (2008). Zn isotopic fractionation caused by sorption on goethite and 2-Lines ferrihydrite. *Geochim. Cosmochim. Acta* 72, 4886–4900. doi: 10.1016/j.gca.2008.07.007

Khatkar, S. P., and Devi, R. (2006). Thioglycolic acid as a reagent for trace determination of Zn(II), Cd(II) and Hg(II). *Asian J. Chem.* 18, 724–726.

Merdzan, V., Domingos, R. F., Monteiro, C. E., Hadioui, M., and Wilkinson, K. J. (2014). The effects of different coatings on zinc oxide nanoparticles and their influence on dissolution and bioaccumulation by the green alga, C. reinhardtii. *Sci. Total Environ.* 488, 316–324. doi: 10.1016/j.scitotenv.2014.04.094

Oriekhova, O., and Stoll, S. (2016). Stability of uncoated and fulvic acids coated manufactured CeO2 nanoparticles in various conditions: from ultrapure to natural Lake Geneva waters. *Sci. Total Environ.* 562, 327–334. doi: 10.1016/j.scitotenv.2016.03.184

Piccinno, F., Gottschalk, F., Seeger, S., and Nowack, B. (2012). Industrial production quantities and uses of ten engineered nanomaterials in Europe and the world. *J. Nanopart Res.* 14, 1–11. doi: 10.1007/s11051-012-1109-9

Pickering, S., Kshirsagar, A., Ruzyllo, J., and Xu, J. (2012). Patterned mist deposition of tri-colour CdSe/ZnS quantum dot films toward RGB LED devices. *Opto Electron. Rev.* 20, 148–152. doi: 10.2478/s11772-012-0019-9

Pinheiro, J. P., and van Leeuwen, H. P. (2004). Scanned stripping chronopotentiometry of metal complexes: lability diagnosis and stability computation. *J. Electroanal. Chem.* 570, 69–75. doi: 10.1016/j.jelechem.2004.03.016

Sivry, Y., Gelabert, A., Cordier, L., Ferrari, R., Lazar, H., Juillot, F., et al. (2014). Behavior and fate of industrial zinc oxide nanoparticles in a carbonate-rich river water. *Chemosphere* 95, 519–526. doi: 10.1016/j.chemosphere.2013.09.110

Soares, H. M. V. M., and Conde, P. C. F. L. (2000). Electrochemical investigations of the effect of N-substituted aminosulfonic acids with a piperazinic ring pH buffers on heavy metal processes which may have implications on speciation studies. *Anal. Chim. Acta* 421, 103–111. doi: 10.1016/S0003-2670(00)01028-X

Spathariotis, E., and Kallianou, C. (2007). Adsorption of copper, zinc, and cadmium on goethite, aluminum−substituted goethite, and a system of kaolinite–goethite: surface complexation modeling. *Commun. Soil Sci. Plant Anal.* 38, 611–635. doi: 10.1080/00103620701216005

Supiandi, I., Charron, G., Tharaud, M., Benedetti, M. F., and Sivry, Y. (2020). Tracing multi-isotopically labelled CdSe/ZnS quantum dots in biological media. *Sci. Rep.* 10:2866. doi: 10.1038/s41598-020-59206-w

Supiandi, N. I., Charron, G., Tharaud, M., Cordier, L., Guigner, J.-M., Benedetti, M. F., et al. (2019). Isotopically labeled nanoparticles at relevant concentrations: how low can we go? the case of CdSe/ZnS QDs in surface waters. *Environ. Sci. Technol.* 53, 2586–2594. doi: 10.1021/acs.est.8b04096

van Leeuwen, H. P., and Town, R. M. (2003). Electrochemical metal speciation analysis of chemically heterogeneous samples:? the outstanding features of stripping chronopotentiometry at scanned deposition potential. *Environ. Sci. Technol.* 37, 3945–3952. doi: 10.1021/es030033p

Yung, M. M. N., Wong, S. W. Y., Kwok, K. W. H., Liu, F. Z., Leung, Y. H., Chan, W. T., et al. (2015). Salinity-dependent toxicities of zinc oxide nanoparticles to the marine diatom *Thalassiosira pseudonana*. *Aquat. Toxicol.* 165, 31–40. doi: 10.1016/j.aquatox.2015.05.015

Zelano, I. O., Sivry, Y., Quantin, C., Gélabert, A., Maury, A., Phalyvong, K., et al. (2016). An isotopic exchange kinetic model to assess the speciation of metal available pool in soil: the case of nickel. *Environ. Sci. Technol.* 50, 12848–12856. doi: 10.1021/acs.est.6b02578

Zhao, L., Hu, L., and Fang, X. (2012). Growth and device application of CdSe nanostructures. *Adv. Funct. Mater.* 22, 1551–1566. doi: 10.1002/adfm.201103088

Conflict of Interest: The authors declare that the research was conducted in the absence of any commercial or financial relationships that could be construed as a potential conflict of interest.